A CLAS Proposal for PAC44

Transition Form Factors of the η' and ϕ Mesons with CLAS12

M. C. Kunkel*†1, M. J. Amaryan[2], D. Lersch[1], J. Ritman†1, S. Schadmand†1, X. Song[1]

[1]Forschungszentrum Jülich, Jülich (Germany)
[2]Old Dominion University (U.S.A.)

Abstract

Dalitz decays are radiative decays in which the photon is virtual and subsequently produces an electron positron pair, $P \to l^+l^- X$. Such decays serve as an important tool used to reveal the internal structure of hadrons and the interaction mechanisms between photons and hadrons. Furthermore, assuming point-like particles, the electromagnetic interaction is calculable within QED by the Kroll-Wada formula. Transition form factors quantify deviations from the QED decay rate. They characterize modifications of the point-like photon-meson vertex due to the structure of the meson. For the η' meson this deviation represents the internal structure of the meson, while for the ϕ meson the deviation represents the transition from $\phi \to \eta$. The transition form factor can be characterized as $\left|F(q^2)\right|$, where q^2 is the square of the invariant mass of the lepton pair, and can be determined by comparing QED predictions to the experimentally measured rate.

Measurements with the highest scientific impact on the determination of the transition form factor have been performed in the space-like region ($q^2 < 0$) in collider experiments. However, due to experimental limitations (e.g. $\pi^\pm$ contamination in lepton sample, low branching fractions, external conversion contamination), transition form factors in the time-like region ($q^2 > 0$) have not yet been precisely determined. Recent measurements of the time-like transition form factor for $\eta' \to e^+e^-\gamma$ have been performed by the BESIII collaboration with insufficient statistical precision, therefore the proper theoretical description cannot be determined.

From previous CLAS analyses using the g12 data set, it was preliminarily shown that measurements of the time-like transition form factor were achievable, but without the statistical precision needed to be competitive. Therefore, we propose to use CLAS12 to focus

---

*Contact person, email: m.kunkel@fz-juelich.de
†Spokesperson

on the dilepton decay channels from the reactions $ep \rightarrow e'p\eta'$ and $ep \rightarrow e'p\phi$, where $\eta' \rightarrow e^+e^-\gamma$ and $\phi \rightarrow \eta e^+e^-$. The CLAS12 detector will be used to identify and measure the e^+e^- decay products by means of the High Threshold Cherenkov Counter (HTCC), Pre-Calorimeter (PCAL) and Electromagnetic Calorimeter (EC). The combination of HTCC+PCAL+EC can provide a rejection factor for single $e^\pm/\pi^\pm$ of up to 10^6 for momenta less than 4.9 GeV/c with $\approx 100\%$ efficiency. For dileptons (e^+e^- pairs), this rejection factor will be $\approx 10^{12}$, which enables dilepton studies for branching ratios $\approx 10^{-9}$. Precise determination of momenta and angles of the e^+e^- decay products are the key features available to CLAS12. The momentum and angle of final state photons will be determined in CLAS12 by using the PCAL and EC. Consequently, the photon in the process $\eta' \rightarrow e^+e^-\gamma$ and the photons in the process $\phi \rightarrow e^+e^-\eta \rightarrow e^+e^-\gamma\gamma$ will be detected. Preliminary studies using the CLAS12 simulation suite have shown that a beam time of 100 days, at full luminosity, will accumulate a data sample at least one order of magnitude larger in statistics than the most current $\eta' \rightarrow e^+e^-\gamma$ and $\phi \rightarrow \eta e^+e^-$ measurement.

1 Introduction

In the year 1951, Richard Dalitz published a letter [1] in which he calculated the rate for the π^0 decaying into an electron-positron pair (dilepton) and a photon, $\pi^0 \rightarrow e^+e^-\gamma$. The calculation assumed that the decay proceeded through a two–photon decay in which one of the photons was virtual and converted internally into an electron-positron pair. This kind of reaction is now known as a Dalitz decay. The experimental evidence of this decay process was first observed in emulsion plates exposed to the Chicago cyclotron in 1952 [2] and a number of experiments performed over the next ten years verified Dalitz's hypothesis that the $\pi^0 \rightarrow e^+e^-\gamma$ decay resulted from internal conversion of a virtual photon [3, 4, 5]. A few years later N. Kroll and W. Wada calculated the framework for Dalitz decays within the QED framework [6], and extended the framework to double Dalitz Decays, in which the π^0 decays into two electron-positron pairs via emission of two virtual photons. Throughout the following years, much work was done to extend the framework of Dalitz decays to heavier mesons, such as η, ω, η', and ϕ. With numerous experimental data taken, it was shown that the shape of the dilepton mass spectrum deviated from the QED predictions. Such deviations are attributed to the meson not being point-like, as calculated in QED, but instead to the internal structure of the meson. The virtual photon, that decayed into a dilepton pair, has the ability to probe the structure of meson because, like its on-shell counterpart, emission of a virtual photon is radiation, which decouples from any strong interaction within the meson when the meson transitions into its decay. Therefore, the information of the transition is encoded into the virtual photon, known as the Transition Form

Factor (TFF), and can be characterized as $\left|F(q^2)\right|$, where q^2 is the square of the invariant mass of the lepton pair. The transition form factor can be determined by comparing QED predictions to the experimentally measured rate.

In this proposal we present an experiment to study two channels of which decay via Dalitz decays, $\eta \to e^+ e^- \gamma$ and $\phi \to e^+ e^- \eta$. The η and ϕ are produced via electro-production, $ep \to ep\eta'$ and $ep \to ep\phi$ in Hall B, using the CLAS12 detector. The superior $e^+ e^-/\pi^+ \pi^-$ discrimination of the CLAS12 detector will give access to measurements for which $e^+ e^-/\pi^+ \pi^-$ branching ratios of 10^{12} is achievable. This proposal is organized as follows. In Section 2 we summarize the current knowledge of Dalitz decays and transition form factors, challenges in dilepton signal quality and how the CLAS12 detector can surpass the current challenges in measuring a TFF of low statistical error. In Section 3, an explanation of the kinematics of the decay processes will be given as well as kinematics of main competing backgrounds. In Section 4 a brief discussion on past CLAS analysis will be given, along with a description of analysis techniques that have been used and will be used in a CLAS12 measurement. Also in Section 4, an explanation of the Monte-Carlo simulations that were performed to extract the acceptances will be given as well as a calculation of expected yield and a validity check on the expected yield from previous CLAS analyses. In Section 5 we present the beam time request and a summary of the experiment.

2 Motivation

Here I will briefly write about the motivation to use dalitz decays to study the structure of meson. I will include the g-2 measurements Previous results etc

3 Kinematics

The main decays studied for this analysis are when a pseudoscalar meson, $P_p(\eta')$, decays via 2 photons $\gamma\gamma$ or a photon γ and a dilepton $(l^+ l^-)$ and when a vector meson $V_p(\phi)$, decays via an η and a photon γ or an η and a dilepton $(l^+ l^-)$. This section will briefly discuss the physics of each decay.

3.1 η' Decays

Figure 1 illustrates the Feynman diagrams for the "Two photon decay" and the "Dalitz decay".
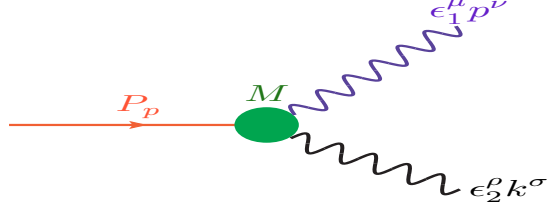
(a)
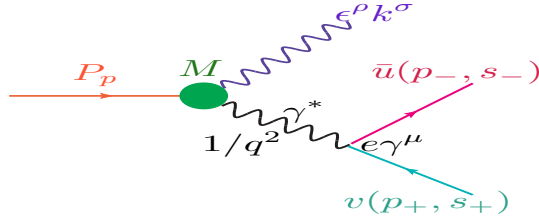
(b)

Figure 1: Feynman diagram of $P_p(\eta')$ two photon decay (a), ϵ_1 and ϵ_2 are the polarizations, p and k are 4-momenta of the photons. Feynman diagram of $P_p(\pi^0)$ Dalitz decay (b), the variable $s_\pm$ are the spin helicities of the outgoing leptons $l^\pm$ with 4-momenta $p_\pm$ and ϵ is the polarization of the outgoing photon with 4-momenta k. In both diagrams $\mathcal{M}$ is the form factor.

3.1.1 $\eta' \to \gamma\gamma$ Decay

As shown in Fig. 1a, the two photon decay can be expressed in terms of the respective momentum, $P_p(\eta') \to \gamma(\epsilon_1, p)\gamma(\epsilon_2, k)$, where ϵ_1 and ϵ_2 are the polarizations of the photons with 4-momenta p and k. Dropping the nomenclature (η') in $P_p(\eta')$, the four momentum of the decaying meson is $P_p = p + k$. Using the Feynman rules as given in [7]and [8], which are Lorentz and gauge invariant and also parity conserving, the amplitude can be solved to be:

$$\mathcal{M}(P_P \to \gamma(\epsilon_1, p)\gamma(\epsilon_2, k)) = M_P(p^2 = 0, k^2 = 0)\varepsilon_{\mu\nu\rho\sigma}\epsilon_1^\mu p^\nu \epsilon_2^\rho k^\sigma \qquad (1)$$

where $\varepsilon_{\mu\nu\rho\sigma}$ is the antisymmetric metric tensor. The form factor, $M_P(p^2 = 0, k^2 = 0)$, contains information of the decaying meson and since the decay products are on-shell photons, which are massless, M_P is a constant given

4

as;

$$
M_P = \begin{cases}
\dfrac{\alpha}{\pi f_\pi} & \text{if } P = \eta'; \\[2ex]
\dfrac{\alpha}{\pi f_\pi}\dfrac{1}{\sqrt{3}}\left(\dfrac{f_\pi}{f_8}\cos\theta_{mix} - 2\sqrt{2}\dfrac{f_\pi}{f_0}\sin\theta_{mix}\right) & \text{if } P = \eta; \\[2ex]
\dfrac{\alpha}{\pi f_\pi}\dfrac{1}{\sqrt{3}}\left(\dfrac{f_\pi}{f_8}\sin\theta_{mix} + 2\sqrt{2}\dfrac{f_\pi}{f_0}\cos\theta_{mix}\right) & \text{if } P = \eta'
\end{cases} \tag{2}
$$

where $\alpha = e^2/4\pi \approx 1/137$ is the fine structure constant, $f_\pi \approx 92.4\,\text{MeV}$ is the physical value of the pion-decay constant and $f_0 \approx 1.04 f_\pi$ and $f_8 \approx 1.3 f_\pi$ are the singlet and octet Pseudo-Goldstone meson decay constants.

3.1.2 *Squared Matrix Element*

The squared matrix element of the decay $P_P \to \gamma(\epsilon_1, p)\gamma(\epsilon_2, k)$ is given by

$$
|\mathcal{M}(P_P \to \gamma(\epsilon_1, p)\gamma(\epsilon_2, k))|^2 = |M_P|^2\, \varepsilon_{\mu\nu\rho\sigma}\varepsilon_{\mu'\nu'\rho'\sigma'}\epsilon_1^\mu p^\nu \epsilon_2^\rho k^\sigma \epsilon_1^{\mu'} p^{\nu'} \epsilon_2^{\rho'} k^{\sigma'} \tag{3}
$$

which can be simplified to;

$$
|\mathcal{M}(P_P \to \gamma(p)\gamma(k))|^2 = |M_P|^2\, \varepsilon_{\mu\nu\rho\sigma}\varepsilon^{\mu\nu}{}_{\rho'\sigma'} p^\rho p^{\rho'} k^\sigma k^{\sigma'} \tag{4}
$$

by assuming that the polarizations of the photons remain unobserved, as they are in CLAS. Therefore the photon polarization vectors can be summed using Eq. 5.75 from [7] which reads as;

$$
\sum_{polarizations} \epsilon_\mu \epsilon_{\mu'} \to -g_{\mu\mu'} \tag{5}
$$

As indicated in [7], the right arrow indicates that this is not an actual equality, but the solution is valid as long as both sides are dotted into Eq. 3. The antisymmetric tensor, $\varepsilon_{\mu\nu\rho\sigma}\varepsilon^{\mu\nu}{}_{\rho'\sigma'}$ is simplified using Eq. A.30 of [7];

$$
\varepsilon_{\mu\nu\rho\sigma}\varepsilon^{\mu\nu}{}_{\rho'\sigma'} = -2(g_{\rho\rho'}g_{\sigma\sigma'} - g_{\rho\sigma'}g_{\rho'\sigma}) \tag{6}
$$

$$
\tag{7}
$$

Applying Eq. 6 to Eq. 4 results in;

$$
|\mathcal{M}(P_P \to \gamma(p)\gamma(k))|^2 = |M_P|^2\,(-2)(p^2 k^2 - (p \cdot k)^2)\,. \tag{8}
$$

Substituting

$$
(p + k)^2 = p^2 + k^2 + 2(p \cdot k)\,, \tag{9}
$$

and applying $p^2 = k^2 = 0$, since both photons are massless because they are on-shell, we can derive the final expression of the squared amplitude of the decay $P_P \to \gamma(\epsilon_1, p)\gamma(\epsilon_2, k)$ as;

$$
|\mathcal{M}(P_P \to \gamma(p)\gamma(k))|^2 = |M_P|^2\,\frac{1}{2}(p + k)^4 = \frac{1}{2}|M_P|^2\, m_P^4 \tag{10}
$$

where m_P^4 is the mass of the η' derived from the 4-momenta conservation equation $(p + k)^4 = m_P^4$

3.1.3   *Decay rate*

The decay rate of a two-body decay is explained in Equation 46.17 of [9] as

$$d\Gamma = \frac{1}{32\pi^2} A \left| \mathcal{M} \right|^2 \frac{|\mathbf{p_1}|}{m_p^2} d\Omega \ , \tag{11}$$

where $d\Omega$ is the solid angle of particle 1 and A is the symmetry factor which appears because of the Bose symmetry of the two outgoing photons. Substituting the square matrix element from Eq. 10 into Eq. 11 and integrating over the solid angle yields;

$$\Gamma_{P \to \gamma\gamma} = \frac{1}{32\pi^2} \frac{1}{2} \left| \mathcal{M}(P_P \to \gamma(p)\gamma(k)) \right|^2 \frac{|\mathbf{p}|}{m_P^2} 4\pi = \frac{1}{32\pi} \left| M_P \right|^2 m_P^2 \left| \mathbf{p} \right| \tag{12}$$

Finally, in the center-of-mass (C.M.) frame of the decaying meson, $\mathbf{p} = \mathbf{E}_\gamma^{\mathbf{C.M.}} = \frac{\mathbf{m_P}}{\mathbf{2}}$, we find the final expression of the decay rate of $P_P \to \gamma(\epsilon_1, p)\gamma(\epsilon_2, k)$ as;

$$\Gamma_{P \to \gamma\gamma} = \frac{1}{64\pi} \left| M_P \right|^2 m_P^3 \ . \tag{13}$$

3.2 $\phi \to \eta\gamma$ **Decay**

The $\phi \to \eta\gamma$ decay is analogous to the $\eta' \to \gamma\gamma$ decay by replacing the initial pseudoscalar meson P_p with a vector meson V_p and one of the γ propagators with η. In this substitution

$$\mathcal{M}(V_P(\epsilon_1) \to \eta(p)\gamma(\epsilon_2, k)) = M_V(p^2 = m_\eta, k^2 = 0)\varepsilon_{\mu\nu\rho\sigma}\epsilon_1^\mu p^\nu \epsilon_2^\rho k^\sigma \tag{14}$$

again, $\varepsilon_{\mu\nu\rho\sigma}$ is the antisymmetric metric tensor and the form factor, $M_V(p^2 = \eta, k^2 = 0)$, contains information of the $\phi - \eta$ transition.

3.2.1   *Decay rate*

The algebra for solving the squared matrix element is similar to Sec. 3.1.2, however since now the initial meson has polarization, a factor of $1/3$ [10] is introduced. The decay rate is also similar within a factor of $1/3$ and can be represented as:

$$\Gamma_{V \to \eta\gamma} = \frac{1}{3} \frac{1}{64\pi} \left| M_V \right|^2 \left(\frac{m_\phi - m_\eta}{m_\phi} \right)^3 \ . \tag{15}$$

3.3   *Photon Conversion to e^+e^- Pairs*

When a photon travels through matter at energies greater than 100 MeV, it can convert into an electron-positron pair. The process of pair production,

$\gamma Z \rightarrow Ze^+e^-$, occurs when a photon with $E_0 > 2m_ec^2$ converts into an electron and a positron. The cross section for this process can be written as;

$$\sigma_{\gamma \rightarrow e^+e^-} = \frac{A}{N_A\rho\lambda_\gamma} \ , \ \lambda_\gamma = \frac{9}{7}X_0 \tag{16}$$

where λ is the interaction length, or mean free path, ρ is the density of the material, N_A is Avogadro's number and A is the atomic mass of the material. The probability of pair production to occur is solely based on X_0, the radiation length of the medium and this probability can be expressed as;

$$\frac{dP}{dx} = \frac{1}{\lambda_\gamma} \exp(\frac{-x}{\lambda_\gamma}) \ . \tag{17}$$

Using the ratio, $\frac{\Gamma_{\eta' \rightarrow e^+e^-\gamma}}{\Gamma_{\eta' \rightarrow \gamma\gamma}} = 2.13 \cdot 10^{-2}$, that has been preliminary measured by CLAS, which is consistent with [11], the probability of pair production when a photon, from the $\eta' \rightarrow \gamma\gamma$ decay, traveling though 5 cm of liquid hydrogen, ℓH_2, is shown in Fig. 2 as well as the number of $\eta' \rightarrow \gamma\gamma \rightarrow e^+e^-\gamma$ / $100\eta' \rightarrow e^+e^-\gamma$. Since CLAS12 has a vertex resolution of ≈ 1 mm the
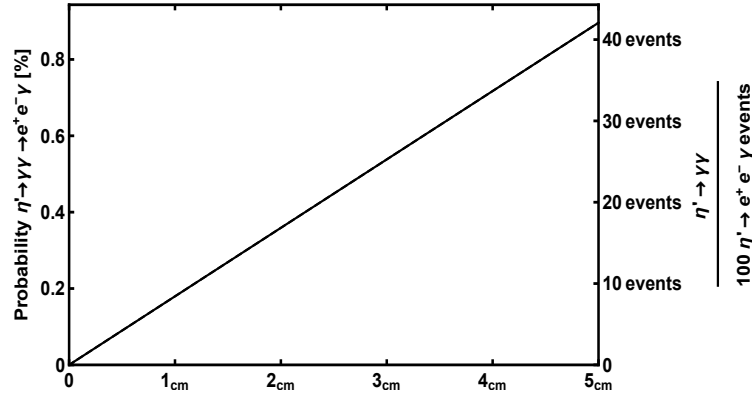

Figure 2: (Left axis)Probability of pair production, $\gamma \rightarrow e^+e^-$; (Right axis) number of $\eta' \rightarrow \gamma\gamma \rightarrow e^+e^-\gamma$ / $100\eta' \rightarrow e^+e^-\gamma$ as a function of distance in liquid hydrogen.

probability of pair production traveling through 10 mm is shown in Fig. 3. Therefore, a 1 mm cut on the primary vertex will yield a contamination of $\approx$ one externally converted e^+e^- from $\eta' \rightarrow \gamma\gamma \rightarrow e^+e^-\gamma$ per Dalitz decays $100\eta' \rightarrow e^+e^-\gamma$ These type of subprocess mimics the Dalitz decay $\eta' \rightarrow e^+e^-\gamma$, described in Sec. 3.4. Since there are two photons with equal probability of conversion for $\eta' \rightarrow \gamma\gamma$, the total probabilities shown is for when either photon externally converts. Using the ratio, $\frac{\Gamma_{\phi \rightarrow e^+e^-\eta}}{\Gamma_{\phi \rightarrow \gamma\eta}} = 9.58 \cdot 10^{-2}$ [9], the probability of pair production when a photon, from the $\phi \rightarrow \gamma\eta$ decay,
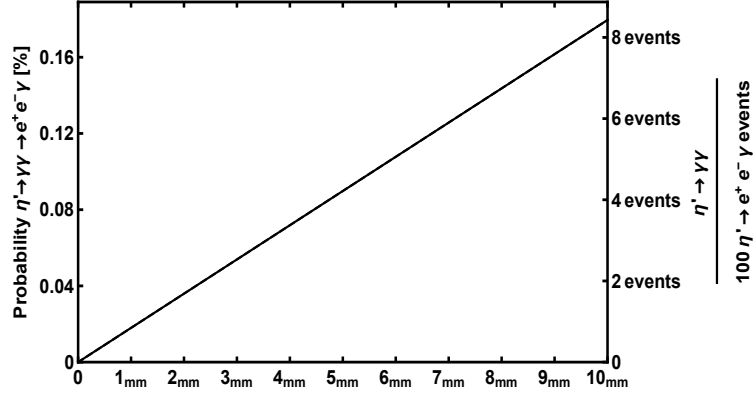
Figure 3: (Left axis)Probability of pair production, $\gamma \to e^+e^-$; (Right axis) number of $\eta' \to \gamma\gamma \to e^+e^-\gamma$ / $100\eta' \to e^+e^-\gamma$ as a function of distance in liquid hydrogen.
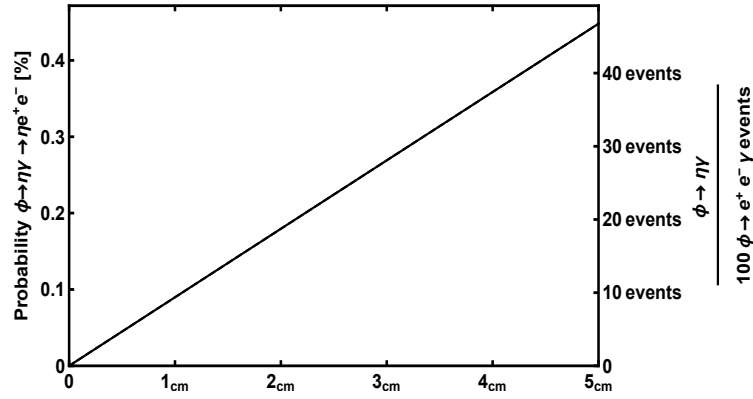

Figure 4: (Left axis)Probability of pair production, $\gamma \to e^+e^-$; (Right axis) number of $\phi \to \gamma\eta \to e^+e^-\eta$ / $100\phi \to e^+e^-\eta$ as a function of distance in liquid hydrogen.

traveling though 5 cm of liquid hydrogen, ℓH_2, is shown in Fig. 4 as well as the number of $\phi \to \gamma\eta \to e^+e^-\eta$ / $100\phi \to e^+e^-\eta$. Since CLAS12 has a vertex resolution of ≈ 1 mm the probability of pair production traveling through 10 mm is shown in Fig. 3. Therefore, a 1 mm cut on the primary vertex will yield a contamination of $\approx$ one externally converted e^+e^- from $\phi \to \gamma\eta \to e^+e^-\eta$ per Dalitz decays $100\eta' \to e^+e^-\eta$

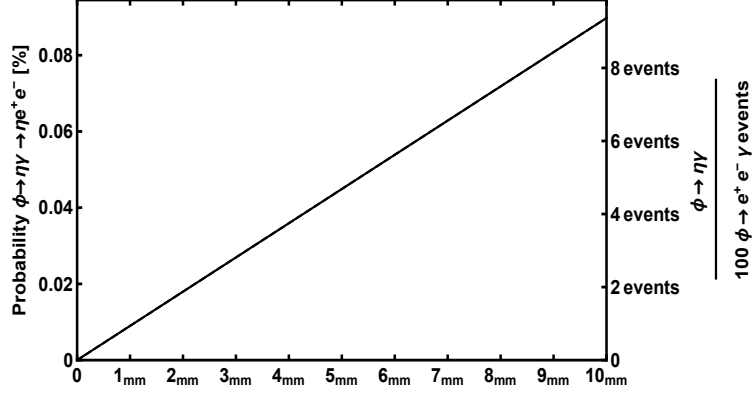Figure 5: (Left axis)Probability of pair production, $\gamma \to e^+e^-$; (Right axis) number of $\phi \to \gamma\eta \to e^+e^-\eta$ / $100\eta' \to e^+e^-\eta$ as a function of distance in liquid hydrogen.

3.4 η' Dalitz Decay

When a pseudoscalar meson decays via a photon γ and a dilepton (l^+l^-) pair, it is known as a Dalitz decay or a so-called single off-shell decay. The Dalitz decay is related to the two photon decay. However, in the Dalitz decay, one of the photons is off-shell (γ^*) and decays into a dilepton pair. Since the Dalitz decay is related to the two photon decay, the form factor of the Dalitz decay, for P(η'), will be similar to the form factor of the two photon decay of P(η'), except there will be an effective mass dependence for the Dalitz decay. Figure 1b depicts the Feymann diagram of the Dalitz decay.

The amplitude for the decay $P_P \to \gamma^\star(p)\gamma(k) \to l^+(p_+)l^-(p_-)\gamma(k)$ is given by the following expression:

$$\mathcal{M}(P \to l^+(p_+,s_+)l^-(p_-,s_-)\gamma) = M_P(p^2, k^2=0)\varepsilon_{\mu\nu\rho\sigma}\frac{1}{q^2}e\bar{u}(p_-,s_-)\gamma^\mu v(p_+,s_-)q^\nu\epsilon^\rho k^\sigma.$$
(18)

Comparing the amplitudes of Eq. 18 and Eq. 1 it is seen that the polarization of the off-shell photon turned into the current $e\bar{u}(p_-,s_-)\gamma^\mu v(p_+,s_-)$ of the lepton pair. The parameters $s_\pm$ are the spin helicities of the outgoing leptons $l^\pm$ and as in Eq. 3, ϵ is the polarization of the outgoing photon.

3.4.1 *Squared Matrix Element*

$$\left|\mathcal{M}(P \to l^+(p_+,s_+)l^-(p_-,s_-)\gamma)\right|^2 =$$
$$\frac{e^2}{q^4}|M|^2\,\varepsilon_{\mu\nu\rho\sigma}\varepsilon_{\mu'\nu'\rho'\sigma'}\bar{u}(p_-,s_-)\gamma^\mu v(p_+,s_+)\bar{v}(p_+,s_+)\gamma^{\mu'}u(p_-,s_-)q^\nu\epsilon^\rho k^\sigma q^{\nu'}\epsilon^{\rho'}k^{\sigma'}.$$
(19)

9

using an equation found between equation 5.3 and 5.4 found in [7]

$$\sum_{s_-,s_+} \bar{u}(p_-,s_-)\gamma^\mu \nu(p_+,s_+)\bar{\nu}(p_+,s_+)\gamma^{\mu'} u(p_-,s_-) = Tr\left[(\not{p}_- + m)\gamma^\mu(\not{p}_+ - m)\gamma^{\mu'}\right]$$

$$= 2q^2\left[-(g_{\mu\mu'} - \frac{p_\mu p_{\mu'}}{q^2}) - \frac{(p_+ - p_-)_\mu(p_+ - p_-)_{\mu'}}{q^2}\right] \tag{20}$$

where the identity $q = p_+ + p_-$ was used. Substituting Eq. 20 into Eq. 19

$$|\mathcal{M}|^2 = \frac{2e^2\,|M_P|^2}{q^2}\varepsilon_{\mu\nu\rho\sigma}\varepsilon_{\mu'\nu'\rho'\sigma'}\left[-g^{\mu\mu'} - \frac{(p_+ - p_-)^\mu(p_+ - p_-)^{\mu'}}{q^2}\right](-g^{\nu\nu'})q^\rho k^\sigma q^{\rho'} k^{\sigma'} \tag{21}$$

Substituting $k = P - q$ and $p_- = q - p_+$ into Eq. 21

$$|\mathcal{M}|^2 = \frac{2e^2\,|M_P|^2}{q^2}\varepsilon_{\mu\nu\rho\sigma}\varepsilon_{\mu'\nu'\rho'\sigma'}\left[-g^{\mu\mu'} - \frac{(2p_+ - q)^\mu(2p_+ - q)^{\mu'}}{q^2}\right]$$

$$\times (-g^{\nu\nu'})(q^\rho P^\sigma - q^\rho q^\sigma)(q^{\rho'}P^{\sigma'} - q^{\rho'}q^{\sigma'}) \tag{22}$$

Applying properties of $-g^{\mu\mu'}$ and $-g^{\nu\nu'}$ onto Eq. 22

$$|\mathcal{M}|^2 = \frac{2e^2\,|M_P|^2}{q^2}\left[\varepsilon_{\mu\nu\rho\sigma}\varepsilon^{\mu\nu}{}_{\rho'\sigma'}q^\rho P^\sigma q^{\rho'}P^{\sigma'} + \frac{4}{q^2}\varepsilon_{\mu\nu\rho\sigma}\varepsilon^\mu{}_{\nu'\rho'\sigma'}p_+^\nu p_+^{\nu'}q^\rho q^{\rho'}P^\sigma P^{\sigma'}\right] \tag{23}$$

Switching to the rest frame of the pseudoscalar meson, P_p, the 4-momenta is transformed to $P^\sigma = m_p\delta^{\sigma 0}$. The squared amplitude of Eq. 23 reads;

$$|\mathcal{M}|^2 = \frac{2e^2\,|M_P|^2}{q^2}m_p^2\left[\varepsilon_{\mu\nu\rho}\varepsilon^{\mu\nu}{}_{\rho'}q^\rho q^{\rho'} - \frac{4}{q^2}\varepsilon_{\mu\nu\rho}\varepsilon^\mu{}_{\nu'\rho'}p_+^\nu p_+^{\nu'}q^\rho q^{\rho'}\right] \tag{24}$$

The sign change is due to $g^{\sigma\sigma'} = -\delta^{\sigma\sigma'}$. Using the antisymmetric tensor properties $\varepsilon_{\mu\nu\rho}\varepsilon^{\mu\nu}{}_{\rho'} = 2\delta_{\rho\rho'}$ and $\varepsilon_{\mu\nu\rho}\varepsilon^\mu{}_{\nu'\rho'} = \delta_{\nu\nu'}\delta_{\rho\rho'} - \delta_{\nu\rho'}\delta_{\rho\nu'} = (\hat{e}_\nu \times \hat{e}_\rho) \cdot (\hat{e}_{\nu'} \times \hat{e}_{\rho'})$, Eq. 24 is reduced to

$$|\mathcal{M}|^2 = \frac{2e^2\,|M_P|^2}{q^2}m_p^2\left[2\,|\mathbf{q}|^2 - \frac{4}{q^2}\,|\mathbf{q}|^2\,|\mathbf{p}_+|^2\sin^2(\theta_{p_+q})\right] \tag{25}$$

3.4.2 Decay rate

The decay rate of a three-body decay is given in Equation 46.19 of [9] as

$$d\Gamma = \frac{1}{(2\pi)^5}\frac{1}{16m_p^2}\,|\mathcal{M}|^2\,|\mathbf{p_1^*}|\,|\mathbf{p_3}|\,d\Omega_1^* d\Omega_3 dm_{12}\ , \tag{26}$$

10

where $(|\mathbf{p_1^*}|, \Omega_1^*)$ is the momentum of particle 1 in the rest frame of 1 and 2, and Ω_3 is the angle of particle 3 in the rest frame of the decaying particle m_p [9]. Relating Eq. 26 to the variables in Eq. 25, where $(|\mathbf{p_1^*}|, \Omega_1^*) = (|\mathbf{p_+}|, \Omega_{p_+q})$, $m_{12} = q$ and $(|\mathbf{p_3}|, \Omega_3) = (|\mathbf{p_k}|, \Omega_k)$, reads;

$$d\Gamma = \frac{1}{(2\pi)^5} \frac{1}{16m_p^2} |\mathcal{M}|^2 |\mathbf{p_+}| |\mathbf{p_k}| \, d\Omega_+ d\Omega_k dq \ , \tag{27}$$

In the rest from of the decaying particle m_p, the 3-momenta $|\mathbf{p_k}| = |\mathbf{q}|$ and the solid angle $\Omega_k = \Omega_q$. Substituting the square matrix element from Eq. 25 into Eq. 27 yields;

$$d\Gamma = \frac{1}{(2\pi)^5} \frac{1}{16m_p^2} \frac{2e^2 |M_P|^2}{q^2} m_p^2 \left[2|\mathbf{q}|^2 - \frac{4}{q^2} |\mathbf{q}|^2 |\mathbf{p_+}|^2 \sin^2(\theta_{p_+q}) \right] |\mathbf{p_+}| |\mathbf{q}| \, d\Omega_{p_+q} d\Omega_q dq \ . \tag{28}$$

The variables $|\mathbf{q}|$ and $|\mathbf{p_+}|$ can be redefined, by means of Eq. 46.20b and Eq. 46.20a of [9], as

$$|\mathbf{q}| = \frac{m_p^2 - q^2}{2m_p} \tag{29}$$

$$|\mathbf{p_+}| = \frac{\sqrt{q^2 - 4m_l^2}}{2} = \frac{q\sqrt{1 - \frac{4m_l^2}{q^2}}}{2} = \frac{q\mathcal{K}}{2} \ , \tag{30}$$

where $\mathcal{K} = \sqrt{1 - \frac{4m_l^2}{q^2}}$. Replacing the variables calculated in Eq. 29 and Eq. 30 into Eq. 28 and collecting terms yields;

$$d\Gamma = \frac{1}{(2\pi)^5} \frac{1}{16m_p^2} |M_P|^2 \left[\frac{2e^2 m_p^2}{8} \left(\frac{m_p^2 - q^2}{2m_p} \right)^3 \right] \left(2 - \mathcal{K}^2 \sin^2(\theta_{p_+q}) \right) \frac{\mathcal{K}}{4q^2} dq^2 d\Omega_{p_+q} d\Omega_q \ , \tag{31}$$

where the identity $qdq = \frac{dq^2}{2}$. Performing the integration of $\Omega_{p_+q} d\Omega_q$ and replacing $e^2 = 4\pi\alpha$ transforms Eq. 31 into;

$$d\Gamma = \frac{1}{(2\pi)^3} \frac{1}{32} \frac{4\pi\alpha}{3} |M_P|^2 \left[\frac{m_p^6 \left(1 - \frac{q^2}{m_p^2} \right)^3}{m_p^3} \right] \left(3 - \mathcal{K}^2 \right) \frac{\mathcal{K}}{q^2} dq^2 \ , \tag{32}$$

which can be simplified further to;

$$d\Gamma = \left(\frac{1}{64\pi} |M_P|^2 m_P^3 \right) \frac{2\alpha}{3\pi} \frac{1}{q^2} \left(1 - \frac{q^2}{m_p^2} \right)^3 \left(1 + \frac{2m_l^2}{q^2} \right) \left(1 - \frac{4m_l^2}{q^2} \right)^{\frac{1}{2}} dq^2 \ . \tag{33}$$

11

It can be seen that the first set of variables in parenthesis in Eq. 33 is Eq. 13, therefore;

$$\frac{d\Gamma}{\Gamma_{\gamma\gamma}dq^2} = \frac{2\alpha}{3\pi}\frac{1}{q^2}\left(1 - \frac{q^2}{m_p^2}\right)^3 \left(1 + \frac{2m_l^2}{q^2}\right)\left(1 - \frac{4m_l^2}{q^2}\right)^{\frac{1}{2}} \qquad (34)$$

which is the Kroll-Wada equation founded in [6].

3.5 ϕ Dalitz Decay

The amplitude for the decay $V_P \rightarrow \gamma^\star(p_1)\eta(p_2) \rightarrow l^+(p_+)l^-(p_-)\eta(p_2)$ is similar Eq. 18, but replacing the on-shell photon with an η:

$$\mathcal{M}(P \rightarrow l^+(p_+,s_+)l^-(p_-,s_-)\eta(p_2)) = M_P(p_1^2,p_2^2)\varepsilon_{\mu\nu\rho\sigma}\frac{1}{q^2}e\bar{u}(p_-,s_-)\gamma^\mu v(p_+,s_-)q^\nu\epsilon^\rho p_2^\sigma. \qquad (35)$$

3.5.1 *Decay rate*

The decay rate for the ϕ transition to $\eta\gamma^\star$ is derived as [12]:

$$\frac{d\Gamma}{\Gamma_{\eta\gamma}dq^2} = \frac{\alpha}{3\pi}\frac{1}{q^2}\left(\left(1 + \frac{q^2}{m_\phi^2 - m_\eta^2}\right)^2 - \frac{4m_\phi^2 q^2}{m_\phi^2 - m_\eta^2}\right)^{\frac{3}{2}}\left(1 + \frac{2m_l^2}{q^2}\right)\left(1 - \frac{4m_l^2}{q^2}\right)^{\frac{1}{2}}, \qquad (36)$$

3.6 Form Factor

The form factor $M_P(p^2, k^2 = 0)$ or $M_P(p_1^2, p_2^2)$ can be written as follows:

$$M_P \rightarrow M_P \times \left|F(q^2)\right|, \qquad (37)$$

where M_p is the decay constant of two photons, for η', as mentioned in Sec. 3.1.1 and $\left|F(q^2)\right|$ is called the transition form factor, which defines the electromagnetic space structure of the meson, therefore for the $\eta' \rightarrow e^+e^-\gamma$ the decay rate modifies as;

$$\frac{d\Gamma}{\Gamma_{\gamma\gamma}dq^2} = \frac{2\alpha}{3\pi}\frac{1}{q^2}\left(1 - \frac{q^2}{m_p^2}\right)^3\left(1 + \frac{2m_l^2}{q^2}\right)\left(1 - \frac{4m_l^2}{q^2}\right)^{\frac{1}{2}}\left|F(q^2)\right|^2, \qquad (38)$$

,which is the Kroll-Wada equation founded in [6], while the $\phi \rightarrow \eta e^+e^-$ decay rate modifies as;

$$\frac{d\Gamma}{\Gamma_{\eta\gamma}dq^2} = \frac{\alpha}{3\pi}\frac{1}{q^2}\left(\left(1 + \frac{q^2}{m_\phi^2 - m_\eta^2}\right)^2 - \frac{4m_\phi^2 q^2}{m_\phi^2 - m_\eta^2}\right)^{\frac{3}{2}}\left(1 + \frac{2m_l^2}{q^2}\right)\left(1 - \frac{4m_l^2}{q^2}\right)^{\frac{1}{2}}\left|F(q^2)\right|^2, \qquad (39)$$

The value of $\left|F(q^2)\right|$ can be directly measured by comparison of the differential cross section with that of Q.E.D. pointlike differential cross section i.e.

$$\frac{d\sigma}{dq^2} = \left[\frac{d\sigma}{dq^2}\right]_{\text{pointlike}} \left|F(q^2)\right|^2 \ ,$$

or by performing a line shape analysis on the l^+l^- invariant system using assumptions on the structure of $\left|F(q^2)\right|$. One such assumption for $\left|F(q^2)\right|$ is the dipole approximation in which

$$F(q^2) = \frac{\Lambda^2(\Lambda^2 + \gamma^2)}{(\Lambda^2 - q^2) + \Lambda^2\gamma^2}$$

where the parameters Λ and γ correspond to the mass and width of the Breit-Wigner shape for the effective contributing vector meson. A first approximation is that $\Lambda \approx M_\rho \approx 0.7$ GeV and $\gamma \approx \Gamma_\rho \approx 0.12$ GeV.

3.7 Summary

The $\gamma\gamma$ decay and the $\gamma^\star\gamma$ decay have different branching ratios as do the decays $\gamma\eta$ decay and the $\gamma^\star\eta$. This difference is attributed to the factor of α along with a q^2 dependence calculated in the Dalitz decay. However, due to the probability of a photon converting into an electron-positron pair in ℓH_2, the total amount of e^+e^- pairs produced via photon conversion can contaminate the measurement of the form factor if primary vertex constraints are not used.

Write the kinematics of dalitz decays, and also of gamma gamma decays. Illustrate how the gamma can externally convert into a e^+e^- pair and discuss how the use of the SVT, with 50-65 μ m can this overcome background since a resolution of 1mm vertex resolution is needed.

4 Measurement

Here I will write about how we plan on using CLAS12

4.1 Previous CLAS6 analysis

4.2 Simulating

Write about using PLUTO++

4.3 Lepton Acceptance

Write about the acceptance

4.4 Calculating Expected Yield

4.4.1 Calculating Virtual Photon Flux

Expected yield

4.5 Realistic Yield

5 Summary

Give beam time request here.

References

[1] R H Dalitz. On an alternative decay process for the neutral π^0-meson. *Proceedings of the Physical Society. Section A*, 64(7):667, 1951.

[2] J. J. Lord, Joseph Fainberg, D. M. Haskin, and Marcel Schein. Narrow angle pairs of particles from nuclear interactions. *Phys. Rev.*, 87:538–539, Aug 1952.

[3] N. P. Samios. Dynamics of internally converted electron-positron pairs. *Phys. Rev.*, 121:275–281, Jan 1961.

[4] P. Lindenfeld, A. Sachs, and J. Steinberger. The Internal Pair Production of γ-Rays of Mesonic Origin; Alternate Modes of π^0 Decay. *Physical Review*, 89:531–537, February 1953.

[5] C. P. Sargent, R. Cornelius, M. Rinehart, L. M. Lederman, and K. Rogers. Diffusion cloud-chamber study of very slow mesons. i. internal pair formation. *Phys. Rev.*, 98:1349–1354, Jun 1955.

[6] Norman M. Kroll and Walter Wada. Internal pair production associated with the emission of high-energy gamma rays. *Phys. Rev.*, 98:1355–1359, Jun 1955.

[7] M.E. Peskin and D.V. Schroeder. *An Introduction to Quantum Field Theory*. Advanced book classics. Addison-Wesley Publishing Company, 1995.

[8] F. Halzen and A.D. Martin. *Quarks and leptons: an introductory course in modern particle physics*. Wiley, 1984.

[9] K.A. Olive et al. Review of particle physics. *Phys. Rev. C*, 38:090001, 2014.

[10] C. Hanhart, A. Kupść, U.-G. Meißner, F. Stollenwerk, and A. Wirzba. Erratum to: Dispersive analysis for $\eta \rightarrow \gamma\gamma^\star$. *The European Physical Journal C*, 75(6):1–3, 2015.

[11] M. Ablikim and et. al. Observation of the dalitz decay $\eta' \rightarrow \gamma e^+ e^-$. *Phys. Rev. D*, 92:012001, Jul 2015.

[12] L.G. Landsberg. Electromagnetic decays of light mesons. *Physics Reports*, 128(6):301 – 376, 1985.